NANO LETTERS

pubs.acs.org/NanoLett

Letter

Volumetric Nanocrystal Lattice Reconstruction through Dynamic Metal Complex Docking

Jiaye Chen, Liangliang Liang,* Shengdong Tan, Shibo Xi, Chun-Ho Lin, Tom Wu, Qian He, and Xiaogang Liu*

Cite This: *Nano Lett.* 2023, 23, 7221−7227

Read Online

ACCESS | Metrics & More | Article Recommendations | Supporting Information

ABSTRACT: Vacancies pose a major challenge in the production of high-quality crystals, particularly at the nanoscale. To address this problem, we report a convenient strategy that involves volumetric lattice reconstruction and dynamic metal complex docking to produce ultrasmall (10 nm) and bright core−shell upconversion nanoparticles (UCNPs). This strategy involves the formation of lanthanide ion−oleic acid complexes during postannealing in solution, which effectively removes vacancies in nanocrystals. The removal of vacancies restricts the diffusion of lanthanide sensitizers and emitters within the core, thus minimizing surface quenching. Our volumetric lattice reconstruction strategy provides fundamental insights into lattice engineering and presents a general strategy for purifying functional nanocrystals for applications in fields such as single-molecule tracking, quantum optics, energy conversion, and others.

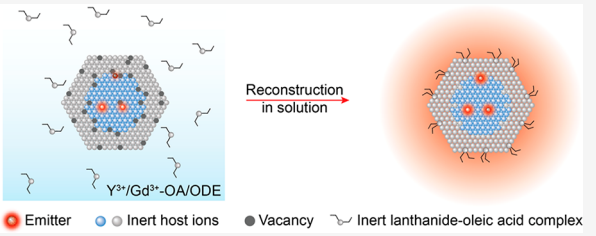

KEYWORDS: *Upconversion nanocrystals, defects, volumetric lattice reconstruction, dynamic metal complex docking, luminescence enhancement*

Lattice defects in crystals can greatly impact their optical and electrical performance.[1−3] Luminescent materials, in particular, are affected by the type, quantity, and distribution of defects. This impact is even more pronounced in nanoscale materials because of luminescence quenching, which complicates the synthesis of small, bright, luminescent nanomaterials. Lanthanide-doped upconversion nanoparticles (UCNPs) are a special type of luminescent nanomaterial with high photostability, long luminescence lifetime, and tunable emission from ultraviolet to near-infrared. Despite their potential applications,[4−13] researchers must use large UCNPs to maintain brightness since defects on the nanoparticle surface can severely quench their luminescence, especially for smaller UCNPs with a much greater surface-to-volume ratio.[14] An inert shell can be applied to nanoparticles to enhance luminescence,[15−17] but the coating process typically leads to a substantial increase in size, which makes it problematic for biological applications. Inherent defects at the core−shell interface and nanoparticle surfaces could still quench luminescence, thereby resulting in limited upconversion enhancement.[18−22] Although approaches, such as dye sensitization,[23−25] surface plasmon coupling,[26] dielectric microlens modulation,[27] and photonic crystal engineering,[28] have been developed to enhance luminescence, they increased the complexity of the process.

Atom diffusion during annealing is a critical process that affects the microstructure and properties of materials.[29−31] The presence of vacancies in nanocrystalline materials can significantly impact the diffusion mechanism. To understand the effect of vacancies on atom diffusion in nanocrystals, we reason that lanthanide complexes could be introduced to interact with the vacancies formed on nanocrystal surfaces. With a proper design, these lanthanide complexes are likely to dock vacancies as they diffuse from the lattice to the surface, thereby resulting in highly crystalline nanocrystals with minimal loss of luminescence intensity (Figure 1).

To verify our speculation, we synthesized ultrasmall $NaGdF_4$:Yb/Tm(49, 1%) UCNPs with a diameter of approximately 6.7 nm and coated them with an inert $NaYF_4$ layer (Figure 2a,b). Despite the enhancement achieved by using the standard core−shell configuration, which increases luminescence intensity by ∼1800-fold at 450 nm (peak intensity), vacancies, especially at the core−shell interface and particle surfaces, remain a major obstacle to further luminescence enhancement (Figure 2f). To remove these vacancies, we postannealed these UCNPs at 300 °C for 1 h in a solution containing yttrium acetate, oleic acid (OA), and 1-octadecene. A further increase in luminescence (116-fold at 450 nm) and quantum yield (29-fold across the whole emission spectra) was observed with well-preserved nanoparticle morphology (Figure

Received: April 30, 2023
Revised: June 12, 2023
Published: June 20, 2023

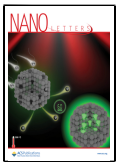

https://doi.org/10.1021/acs.nanolett.3c01621
Nano Lett. 2023, 23, 7221−7227

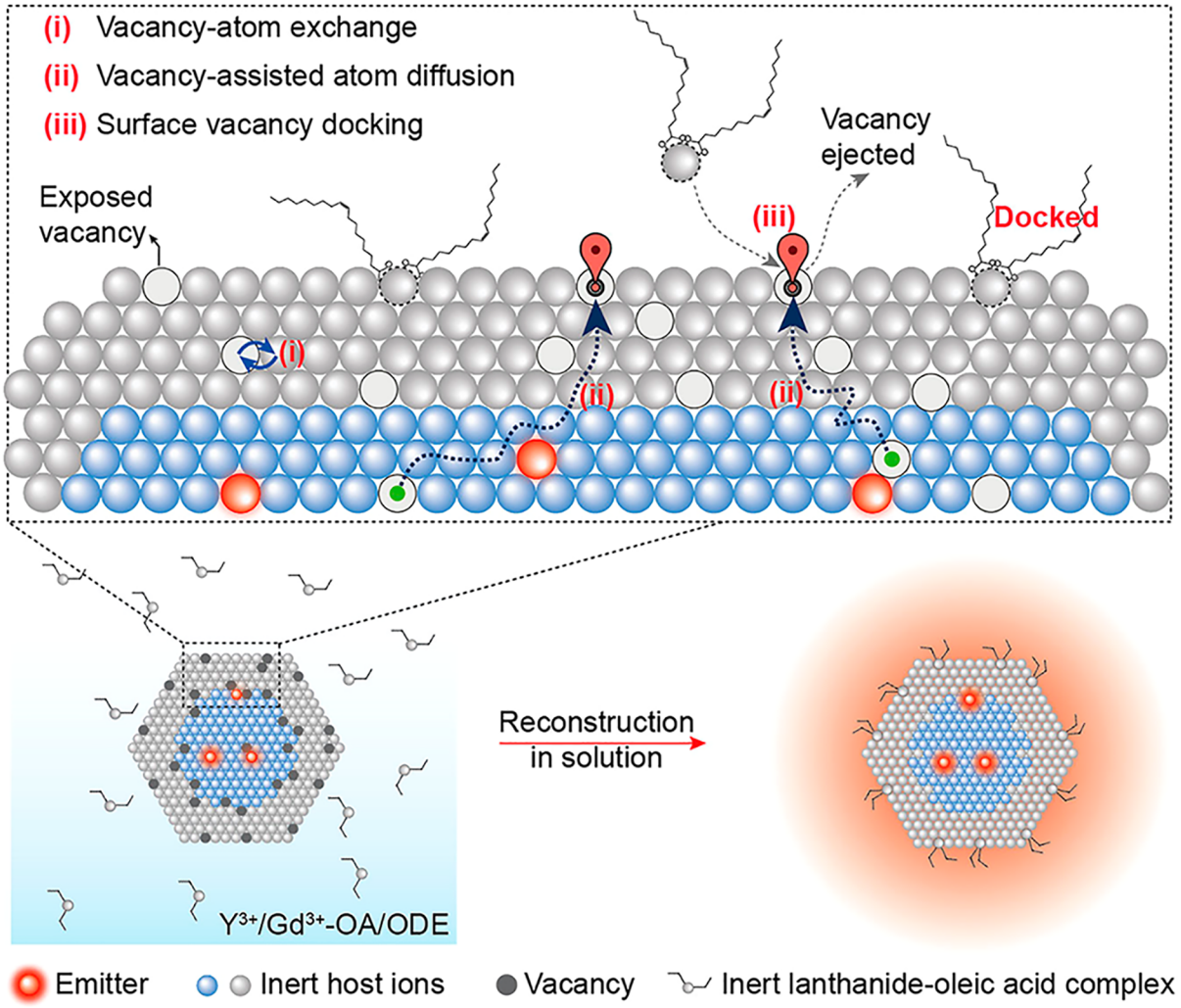

Figure 1. Schematic illustration of volumetric nanocrystal lattice reconstruction through dynamic metal complex docking. Under high-temperature annealing, atoms within crystals can overcome potential barriers and subsequently occupy surrounding vacancies (i). This continuous motion results in vacancy-assisted atom diffusion (ii). By effectively blocking vacancies that diffuse to the surface, the number of defects within the nanocrystal can be significantly reduced, thereby enhancing its luminescent performance (iii).

2c,e,g, and Figures S1 and S2). No increase in luminescence was found in the absence of yttrium acetate, thereby indicating that the inclusion of Y^{3+}−oleic acid complexes is critical for luminescence enhancement (Figure 2d,g). Moreover, Y^{3+}-assisted solution annealing extends the luminescence lifetime from 0.10 to 0.41 ms, thereby signifying effective elimination of defect-induced quenching (Figure 2h, Figure S3a).

For UCNPs with core−shell configuration, a thicker passivation layer provides better protection against surface quenching, which results in higher luminescence (Figure 3a).[32] In contrast, our solution annealing technique with Y^{3+}−OA complexes is highly efficient and requires only a 1 nm passivation layer. A thicker layer of 2 nm showed only slight improvement in luminescence (Figure 3a and Figures S4 and S5a). Reconstruction of volumetric defects extended the luminescence lifetime of core−shell UCNPs with different shell thicknesses to a similar value of ∼0.42 ms (Figure 3b, Figure S3b,c).

As with Y^{3+}, Gd^{3+} is also known for its optical inertness and is commonly utilized for surface passivation.[33] The introduction of Gd^{3+} ions through lattice reconstruction resulted in a noticeable enhancement in upconversion luminescence (Figure 3c). However, the performance of the Gd^{3+}-based complex was found to be slightly inferior to that of the Y^{3+}-based complex because of energy dissipation through Tm^{3+} to Gd^{3+} sublattice.[34]

Heavy Yb^{3+} doping in nanoparticles typically enhances their absorption capacity but can also lead to unwanted energy transfer to surface quenchers, thereby resulting in energy loss. Therefore, a thick passivation layer is required to protect the absorbed energy and prevent its migration to surface quenchers (Figure 3d).[35] Surprisingly, lattice reconstruction with Y^{3+} ions improves the resistance to quenching in Yb^{3+} sensitizers, which results in a ∼1700-fold enhancement in heavily Yb^{3+}-doped UCNPs (Figure 3d and Figure S5b,c). Multilayer configurations ($NaGdF_4$@$NaGdF_4$:Yb_x/Tm_1@$NaYF_4$; x = 19%, 59%, or 99%) were used to maintain consistency in sample size. Notably, even when nanoparticles were dispersed in polar solvents (e.g., water and ethanol), after postannealing, significant fluorescence enhancement was detected, thereby making them attractive for bioapplications (Figure S6). Upconversion enhancement was also observed in samples activated with Er^{3+} (Figure S7).

The regulation of volumetric vacancies has a direct impact on crystallinity. Post-treatment with Y^{3+}−OA complexes resulted in sharp X-ray diffraction patterns, which indicated enhanced crystallinity (Figure 4a). The improvement was limited in the

https://doi.org/10.1021/acs.nanolett.3c01621
Nano Lett. 2023, 23, 7221−7227

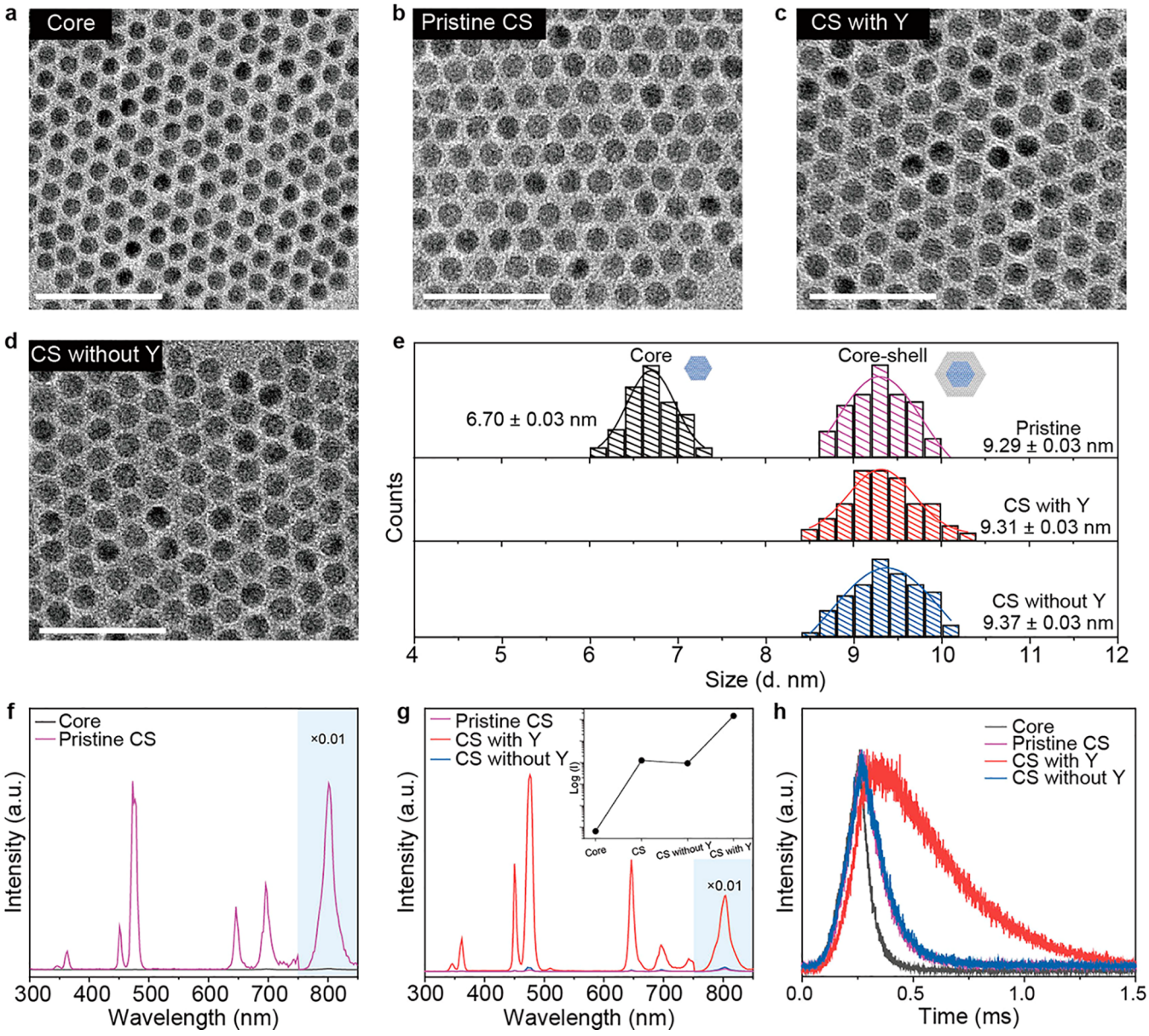

Figure 2. Significant upconversion luminescence enhancement through volumetric lattice purification of sub-10 nm core−shell UCNPs. Transmission electron microscopy (TEM) images of the $NaGdF_4$:Yb/Tm core nanoparticles (a), the pristine $NaGdF_4$:Yb/Tm@$NaYF_4$ core−shell nanoparticles (b), and the $NaGdF_4$:Yb/Tm@$NaYF_4$ core−shell nanoparticles annealed with (c) and without (d) Y^{3+}. Scale bar: 50 nm. (e) The corresponding histogram size distributions of nanocrystals. (f) Upconversion emission spectra of $NaGdF_4$:Yb/Tm and $NaGdF_4$:Yb/Tm@$NaYF_4$ core−shell nanoparticles under 980 nm excitation (4 W cm^{-2}). (g) Upconversion emission spectra of pristine $NaGdF_4$:Yb/Tm@$NaYF_4$ core−shell nanoparticles and those annealed with and without Y^{3+} under 980 nm excitation (4 W cm^{-2}). Inset: Emission intensity of Tm^{3+} at the wavelength of 450 nm. (h) Dynamic curves of Tm^{3+} at 450 nm ($^1D_2 \rightarrow {}^3F_4$) for samples a−d, respectively.

absence of Y^{3+}−OA complexes. Moreover, the use of lanthanide complexes during postannealing led to a blue shift of Raman peaks, thereby indicating a reduction in defects and bond length (Figure S8).[36] Furthermore, extended X-ray absorption fine structure spectroscopy revealed that the coordination number of Yb^{3+} increased after postannealing with lanthanide complexes (Figure 4b), while the coordination number decreased without the complexes, likely because of diffusion of Yb^{3+} into the shell layer (Figure S9 and Table S1). Notably, the successful insertion of Y^{3+} ions into the crystal lattice was directly evidenced by the increased Y^{3+} content after the Y^{3+}−OA post-treatment (Table S2).

Aberration-corrected scanning transmission electron microscopy (STEM) was employed to probe annealing-induced lattice evolution at the single-particle level (Figure 4c−e and Figure S10). High-angle annular dark-field (HAADF) imaging at relatively low magnification showed that annealing treatment with Y^{3+}−OA complexes preserved the core−shell structure well and exhibited a clearly differentiated core−shell contrast (Figure 4d). However, the contrast disappeared without the complexes (Figure 4e). X-ray energy dispersive spectroscopy (X-EDS) of a single nanoparticle also confirmed the strong diffusion of Yb^{3+} ions from the core to the shell in the absence of Y^{3+} (inset, Figure 4e).[37,38] Taken together, these results suggest that the addition of lanthanide complexes during postannealing not only

https://doi.org/10.1021/acs.nanolett.3c01621
Nano Lett. 2023, 23, 7221−7227

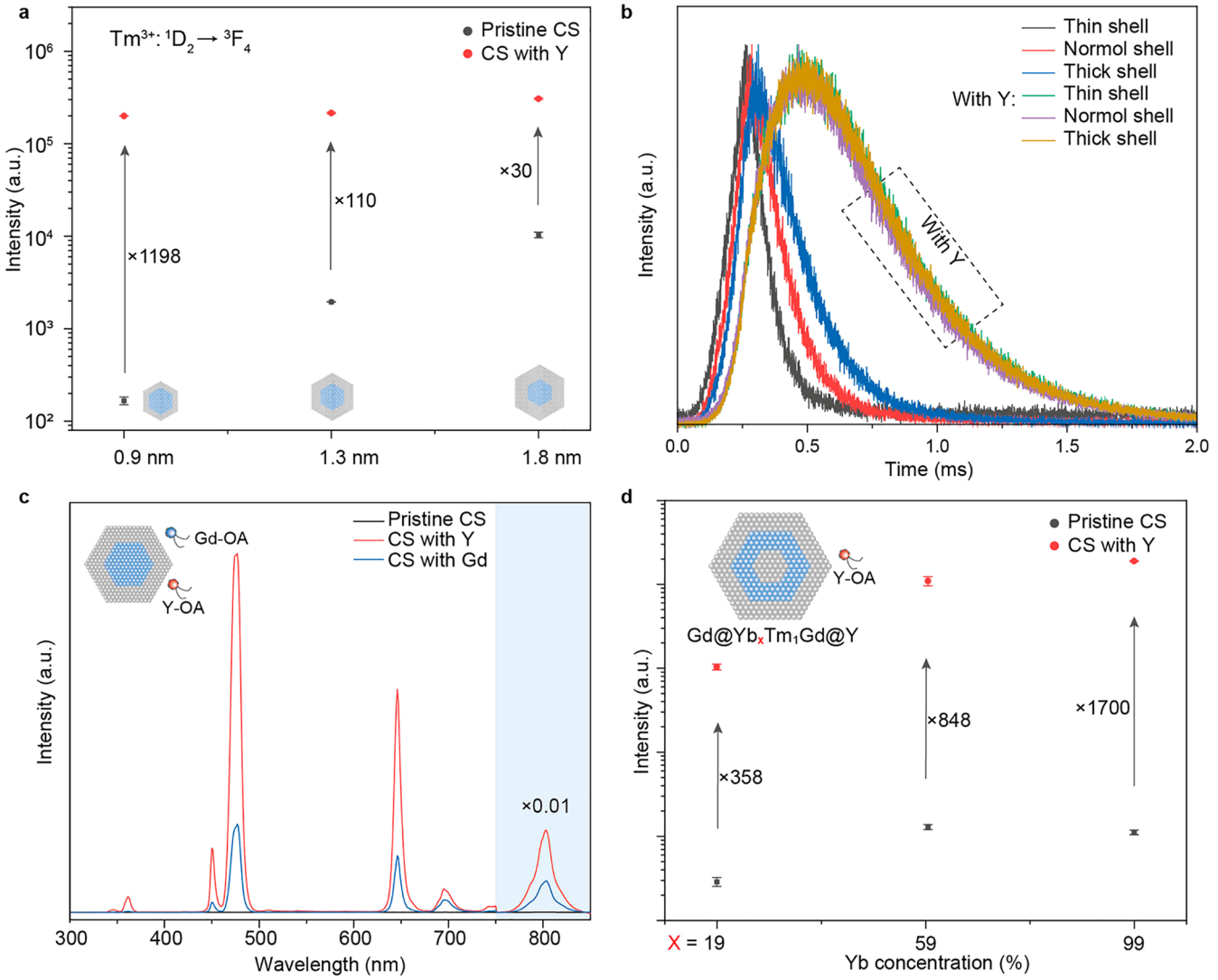

Figure 3. In-depth experimental investigations on upconversion luminescence enhancement through inert lanthanide ion-assisted volumetric lattice purification. (a) Upconversion luminescence enhancement factors of $NaGdF_4$:Yb/Tm@$NaYF_4$ core−shell nanoparticles with different inert shell thicknesses under 980 nm excitation (4 W cm^{-2}) compared with core nanoparticles ($NaGdF_4$:Yb/Tm). (b) Dynamic curves of Tm^{3+} at 450 nm ($^1D_2$ → $^3F_4$) for samples with different inert shell thicknesses. (c) Upconversion emission spectra of pristine $NaGdF_4$:Yb/Tm@$NaYF_4$ core−shell nanoparticles and those annealed with Y^{3+} and Gd^{3+}. (d) Luminescence enhancement factors of $NaGdF_4$@$NaGdF_4$:Yb/Tm@$NaYF_4$ core−shell−shell nanoparticles with different Yb^{3+} concentrations under 980 nm excitation (4 W cm^{-2}).

facilitates the removal of vacancies in nanoparticles but also effectively suppresses ion diffusion, which allows for effective preservation of activators in the core region.

The volumetric lattice purification process was further studied with Monte Carlo simulations on the basis of the model of vacancy-assisted atom diffusion in a solid (Figure 4f−i and Movie S1). The simulations showed a concentration of vacancies at the core−shell interface and particle surfaces (Figure 4f). Without surface docking, these vacancies would participate in ion diffusion during annealing, thereby leading to random distribution in nanoparticles and substantial core−shell intermixing (top panels, Figure 4g−i). In contrast, when lanthanide complexes were added, surface vacancies could be quickly docked by the lanthanide complexes. This leads to the purification of the whole lattice and the suppression of core−shell intermixing (bottom panels, Figure 4g−i).

In summary, by introducing inert lanthanide complexes, we have successfully established a simple and robust strategy that can increase upconversion luminescence by three orders of magnitude on the basis of conventional core−shell UCNPs. Our strategy enables the efficient purification of volumetric lattices and the elimination of ion diffusion while maintaining the same size. In addition to developing sub-10 nm UCNPs with ultrahigh brightness, our study has also provided new insight into crystal defect engineering. Moreover, our unique lattice reconstruction strategy can be easily combined with other approaches, such as organic dye sensitization and excitation energy localization, to further enhance luminescence and can be usefully applied to other luminescent nanophosphors, such as quantum dots and perovskite nanocrystals. This approach is not restricted to luminescent nanomaterials and provides a reliable route to fabricate high-quality functional nanocrystals for various emerging applications, including catalysis, photovoltaics, lighting, and more.

https://doi.org/10.1021/acs.nanolett.3c01621
Nano Lett. 2023, 23, 7221−7227

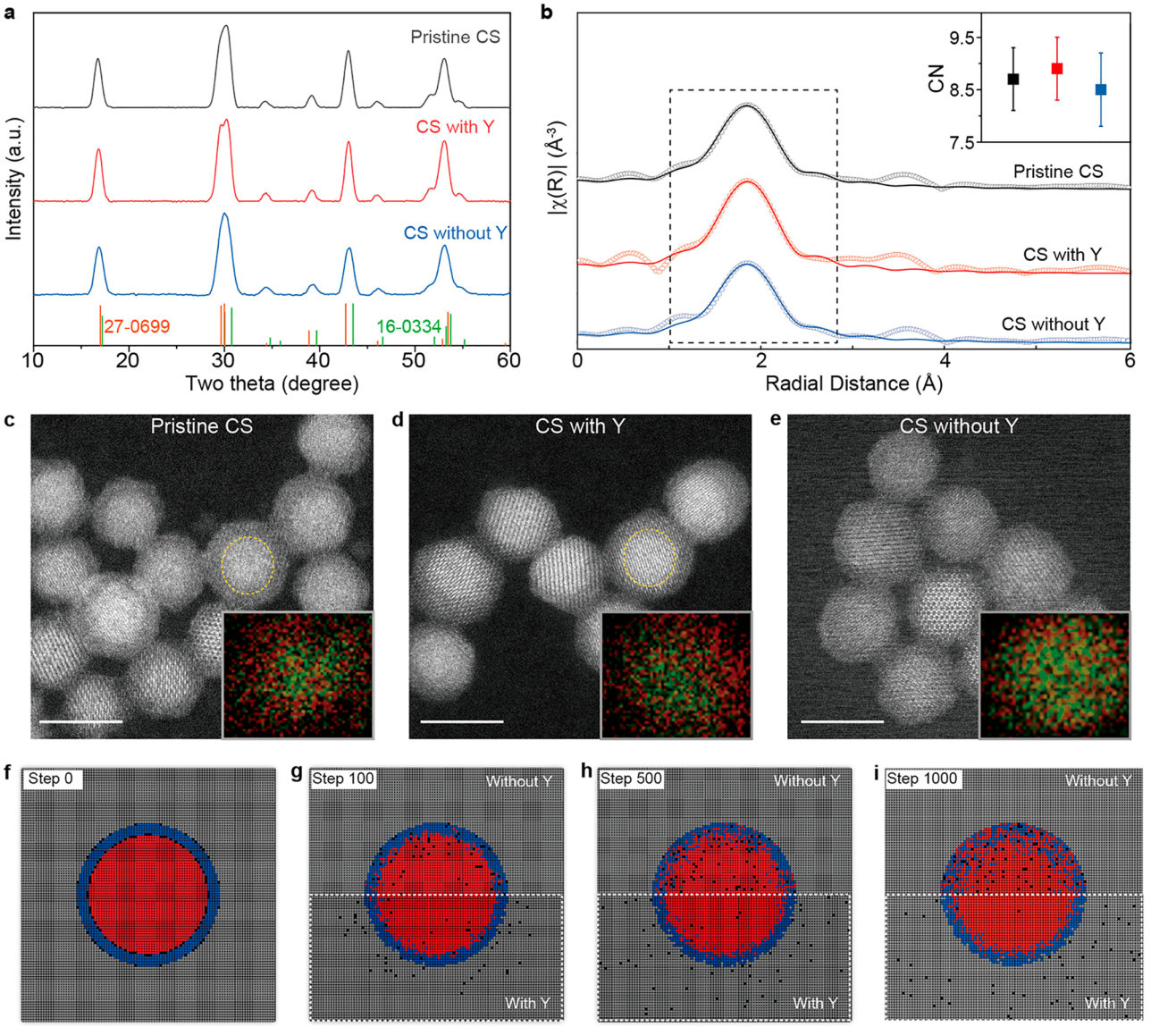

Figure 4. Mechanistic investigations of volumetric lattice purification for significant upconversion luminescence enhancement. (a) X-ray diffraction patterns of core−shell nanocrystals. (b) Experimental (dots) and the fitting (solid lines) results of Fourier transform of Yb−L_3 edge k^2-weighted EXAFS spectra. The window represents the fitting range ($1.5 \leq R \leq 2.85$ Å). Inset: Calculated coordination numbers of Yb^{3+} in Yb−F shell. (c−e) Relatively low-magnification STEM-HAADF images of pristine core-shell UCNPs (c) and those annealed with (d) and without Y (e), respectively. The Yb-enriched core regions are bounded by the dashed ellipse. Inset: X-EDS elemental maps of Y (red) and Yb (green) of individual core−shell nanocrystals in each case. Scale bar: 10 nm. (f−i), Vacancy-assisted atom diffusion simulation for core−shell upconversion nanocrystals before (f) and after diffusion for 100 (g), 500 (h), and 1000 steps (i).

■ ASSOCIATED CONTENT

Supporting Information

The Supporting Information is available free of charge at https://pubs.acs.org/doi/10.1021/acs.nanolett.3c01621.

Additional experimental details, simulation details, and other characterization results (PDF)

Dynamic modeling of lattice reconstruction through dynamic metal complex docking (MP4)

■ AUTHOR INFORMATION

Corresponding Authors

Liangliang Liang − *Department of Chemistry, National University of Singapore, 117543, Singapore*; Email: chmliang@nus.edu.sg

Xiaogang Liu − *Department of Chemistry, National University of Singapore, 117543, Singapore; Institute of Materials Research and Engineering, Agency for Science, Technology and Research, 117602, Singapore*; orcid.org/0000-0003-2517-5790; Email: chmlx@nus.edu.sg

Authors

Jiaye Chen − *Department of Chemistry, National University of Singapore, 117543, Singapore*

Shengdong Tan − *Department of Materials Science and Engineering, National University of Singapore, 117575, Singapore*

Shibo Xi − *Institute of Sustainability for Chemicals, Energy and Environment (ISCE²), Agency for Science, Technology and Research (A*STAR), 627833, Singapore*

https://doi.org/10.1021/acs.nanolett.3c01621
Nano Lett. 2023, 23, 7221−7227

Chun-Ho Lin − *School of Materials Science and Engineering, UNSW, Sydney, NSW 2052, Australia;* orcid.org/0000-0003-0882-4728

Tom Wu − *School of Materials Science and Engineering, UNSW, Sydney, NSW 2052, Australia; Department of Applied Physics, The Hong Kong Polytechnic University, Kowloon 999077 Hong Kong, China*

Qian He − *Department of Materials Science and Engineering, National University of Singapore, 117575, Singapore*

Complete contact information is available at: https://pubs.acs.org/10.1021/acs.nanolett.3c01621

Author Contributions

J.C., L.L., and X.L. conceived the study. T.W., Q.H., and X.L. supervised the project and led the collaboration efforts. J.C. and L.L. designed the upconversion nanoparticles and conducted the optical characterizations. J.C., S.T., S.X., and C.L. performed advanced structural characterization. L.L. did vacancy-assisted atom diffusion simulation. J.C., L.L., and X.L. contributed to the preparation of the manuscript. All authors precipitated in the discussion.

Notes

The authors declare no competing financial interest.

■ ACKNOWLEDGMENTS

This work was supported by National Research Foundation; the Prime Minister's Office of Singapore under its NRF Investigatorship Programme (award no. NRF-NRFI05-2019-0003); and the RIE2025 Manufacturing, Trade and Connectivity (MTC) Programmatic Fund (Award No. M21J9b0085).

■ REFERENCES

(1) Nowotny, M. K.; Sheppard, L. R.; Bak, T.; Nowotny, J. Defect Chemistry of Titanium Dioxide. Application of Defect Engineering in Processing of TiO_2-Based Photocatalysts. *J. Phys. Chem. C* **2008**, *112*, 5275−5300.

(2) Han, T. H.; Tan, S.; Xue, J.; Meng, L.; Lee, J. W.; Yang, Y. Interface and Defect Engineering for Metal Halide Perovskite Optoelectronic Devices. *Adv. Mater.* **2019**, *31*, 1803515.

(3) Saniepay, M.; Mi, C.; Liu, Z.; Abel, E. P.; Beaulac, R. Insights into the Structural Complexity of Colloidal CdSe Nanocrystal Surfaces: Correlating the Efficiency of Nonradiative Excited-State Processes to Specific Defects. *J. Am. Chem. Soc.* **2018**, *140*, 1725−1736.

(4) Liu, Y.; Lu, Y.; Yang, X.; Zheng, X.; Wen, S.; Wang, F.; Vidal, X.; Zhao, J.; Liu, D.; Zhou, Z.; Ma, C.; Zhou, J.; Piper, J. A.; Xi, P.; Jin, D. Amplified Stimulated Emission in Upconversion Nanoparticles for Super-Resolution Nanoscopy. *Nature* **2017**, *543*, 229−233.

(5) Liang, Y.; Zhu, Z.; Qiao, S.; Guo, X.; Pu, R.; Tang, H.; Liu, H.; Dong, H.; Peng, T.; Sun, L. D.; Widengren, J.; Zhan, Q. Migrating Photon Avalanche in Different Emitters at the Nanoscale Enables 46th-Order Optical Nonlinearity. *Nat. Nanotechnol.* **2022**, *17*, 524−530.

(6) Haase, M.; Schäfer, H. Upconverting Nanoparticles. *Angew. Chem., Int. Ed.* **2011**, *50*, 5808−5829.

(7) Jaque, D.; Vetrone, F. Luminescence Nanothermometry. *Nanoscale* **2012**, *4*, 4301−4326.

(8) Zheng, B.; Fan, J.; Chen, B.; Qin, X.; Wang, J.; Wang, F.; Deng, R.; Liu, X. Rare-Earth Doping in Nanostructured Inorganic Materials. *Chem. Rev.* **2022**, *122*, 5519−5603.

(9) Hemmer, E.; Acosta-Mora, P.; Mendez-Ramos, J.; Fischer, S. Optical Nanoprobes for Biomedical Applications: Shining a Light on Upconverting and Near-infrared Emitting Nanoparticles for Imaging, Thermal Sensing, and Photodynamic Therapy. *J. Mater. Chem. B* **2017**, *5*, 4365−4392.

(10) Wisser, M. D.; Fischer, S.; Siefe, C.; Alivisatos, A. P.; Salleo, A.; Dionne, J. A. Improving Quantum Yield of Upconverting Nanoparticles in Aqueous Media via Emission Sensitization. *Nano Lett.* **2018**, *18*, 2689−2695.

(11) Liu, S.; Yan, L.; Huang, J.; Zhang, Q.; Zhou, B. Controlling Upconversion in Emerging Multilayer Core−Shell Nanostructures: From Fundamentals to Frontier Applications. *Chem. Soc. Rev.* **2022**, *51*, 1729−1765.

(12) Brites, C. D.; Balabhadra, S.; Carlos, L. D. Lanthanide-Based Thermometers: At the Cutting-Edge of Luminescence Thermometry. *Adv. Opt. Mater.* **2019**, *7*, 1801239.

(13) Liu, Y.; Tu, D.; Zhu, H.; Chen, X. Lanthanide-Doped Luminescent Nanoprobes: Controlled Synthesis, Optical Spectroscopy, and Bioapplications. *Chem. Soc. Rev.* **2013**, *42*, 6924−6958.

(14) Wang, F.; Wang, J.; Liu, X. Direct Evidence of a Surface Quenching Effect on Size-Dependent Luminescence of Upconversion Nanoparticles. *Angew. Chem., Int. Ed.* **2010**, *49*, 7456−60.

(15) Wurth, C.; Fischer, S.; Grauel, B.; Alivisatos, A. P.; Resch-Genger, U. Quantum Yields, Surface Quenching, and Passivation Efficiency for Ultrasmall Core/Shell Upconverting Nanoparticles. *J. Am. Chem. Soc.* **2018**, *140*, 4922−4928.

(16) Ostrowski, A. D.; Chan, E. M.; Gargas, D. J.; Katz, E. M.; Han, G.; Schuck, P. J.; Milliron, D. J.; Cohen, B. E. Controlled Synthesis and Single-Particle Imaging of Bright, Sub-10 nm Lanthanide-Doped Upconverting Nanocrystals. *ACS Nano* **2012**, *6*, 2686−2692.

(17) Dong, H.; Sun, L. D.; Li, L. D.; Si, R.; Liu, R.; Yan, C. H. Selective Cation Exchange Enabled Growth of Lanthanide Core/Shell Nanoparticles with Dissimilar Structure. *J. Am. Chem. Soc.* **2017**, *139*, 18492−18495.

(18) Xue, M.; Zhu, X.; Qiu, X.; Gu, Y.; Feng, W.; Li, F. Highly Enhanced Cooperative Upconversion Luminescence through Energy Transfer Optimization and Quenching Protection. *ACS Appl. Mater. Interfaces* **2016**, *8*, 17894−901.

(19) Johnson, N. J.; He, S.; Diao, S.; Chan, E. M.; Dai, H.; Almutairi, A. Direct Evidence for Coupled Surface and Concentration Quenching Dynamics in Lanthanide-Doped Nanocrystals. *J. Am. Chem. Soc.* **2017**, *139*, 3275−3282.

(20) Ma, C.; Xu, X.; Wang, F.; Zhou, Z.; Wen, S.; Liu, D.; Fang, J.; Lang, C. I.; Jin, D. Probing the Interior Crystal Quality in the Development of More Efficient and Smaller Upconversion Nanoparticles. *J. Phys. Chem. Lett.* **2016**, *7*, 3252−8.

(21) Mei, S.; Zhou, J.; Sun, H. T.; Cai, Y.; Sun, L. D.; Jin, D.; Yan, C. H. Networking State of Ytterbium Ions Probing the Origin of Luminescence Quenching and Activation in Nanocrystals. *Adv. Sci.* **2021**, *8*, 2003325.

(22) Hu, Y.; Shao, Q.; Dong, Y.; Jiang, J. Energy Loss Mechanism of Upconversion Core/Shell Nanocrystals. *J. Phys. Chem. C* **2019**, *123*, 22674−22679.

(23) Garfield, D. J.; Borys, N. J.; Hamed, S. M.; Torquato, N. A.; Tajon, C. A.; Tian, B.; Shevitski, B.; Barnard, E. S.; Suh, Y. D.; Aloni, S.; Neaton, J. B.; Chan, E. M.; Cohen, B. E.; Schuck, P. J. Enrichment of Molecular Antenna Triplets Amplifies Upconverting Nanoparticle Emission. *Nat. Photonics* **2018**, *12*, 402−407.

(24) Zou, W.; Visser, C.; Maduro, J. A.; Pshenichnikov, M. S.; Hummelen, J. C. Broadband Dye-Sensitized Upconversion of Near-infrared Light. *Nat. Photonics* **2012**, *6*, 560−564.

(25) Chen, G.; Damasco, J.; Qiu, H.; Shao, W.; Ohulchanskyy, T. Y.; Valiev, R. R.; Wu, X.; Han, G.; Wang, Y.; Yang, C.; Ågren, H.; Prasad, P. N. Energy-Cascaded Upconversion in an Organic Dye-Sensitized Core/Shell Fluoride Nanocrystal. *Nano Lett.* **2015**, *15*, 7400−7407.

(26) Wu, Y.; Xu, J.; Poh, E. T.; Liang, L.; Liu, H.; Yang, J. K. W.; Qiu, C. W.; Vallée, R. A. L.; Liu, X. Upconversion Superburst with Sub-2 μs Lifetime. *Nat. Nanotechnol.* **2019**, *14*, 1110−1115.

(27) Liang, L.; Teh, D. B.; Dinh, N.-D.; Chen, W.; Chen, Q.; Wu, Y.; Chowdhury, S.; Yamanaka, A.; Sum, T. C.; Chen, C. H.; Thakor, N. V.; All, A. H.; Liu, X. Upconversion Amplification through Dielectric Superlensing Modulation. *Nat. Commun.* **2019**, *10*, 1391.

(28) Mao, C.; Min, K.; Bae, K.; Cho, S.; Xu, T.; Jeon, H.; Park, W. Enhanced Upconversion Luminescence by Two-Dimensional Photonic Crystal Structure. *ACS Photonics* **2019**, *6*, 1882−1888.

(29) Min, Q.; Zhao, L.; Qi, Y.; Lei, J.; Chen, W.; Xu, X.; Zhou, D.; Qiu, J.; Yu, X. Modified Surface States of $NaGdF_4$:Yb^{3+}/Tm^{3+} up-Conversion Nanoparticles via a Post-Chemical Annealing Process. *Nanoscale* **2018**, *10*, 19031−19038.
(30) Rauls, E.; Frauenheim, T.; Gali, A.; Deák, P. Theoretical Study of Vacancy Diffusion and Vacancy-Assisted Clustering of Antisites in SiC. *Phys. Rev. B* **2003**, *68*, 155208.
(31) Lei, J.; Guo, X.; Min, Q.; Yang, L.; Yang, Q.; Wang, C.; Luo, H.; Yu, X.; Qiu, J.; Zhan, Q.; Xu, X. Brightening Upconverting Nanocrystals Using Laser-Induced Surface Reconstruction. *Mater. Today Nano* **2019**, *8*, 100055.
(32) Xu, X.; Zhou, Z.; Liu, Y.; Wen, S.; Guo, Z.; Gao, L.; Wang, F. Optimising Passivation Shell Thickness of Single Upconversion Nanoparticles Using a Time-Resolved Spectrometer. *APL Photonics* **2019**, *4*, 026104.
(33) Su, Q.; Wei, H. L.; Liu, Y.; Chen, C.; Guan, M.; Wang, S.; Su, Y.; Wang, H.; Chen, Z.; Jin, D. Six-Photon Upconverted Excitation Energy Lock-in for Ultraviolet-C Enhancement. *Nat. Commun.* **2021**, *12*, 4367.
(34) Wang, F.; Deng, R.; Wang, J.; Wang, Q.; Han, Y.; Zhu, H.; Chen, X.; Liu, X. Tuning Upconversion through Energy Migration in Core-Shell Nanoparticles. *Nat. Mater.* **2011**, *10*, 968−73.
(35) Wang, Z.; Meijerink, A. Concentration Quenching in Upconversion Nanocrystals. *J. Phys. Chem. C* **2018**, *122*, 26298−26306.
(36) Kim, H. S.; Kim, Y. J.; Son, Y. R.; Pham, V. N.; Kim, K. J.; Kim, C. W.; Youn, Y. S.; Kwon, O. H.; Lee, H. Verifying the Relationships of Defect Site and Enhanced Photocatalytic Properties of Modified ZrO_2 Nanoparticles Evaluated by in-Situ Spectroscopy and STEM-EELS. *Sci. Rep.* **2022**, *12*, 11295.
(37) Liu, L.; Li, X.; Fan, Y.; Wang, C.; El-Toni, A. M.; Alhoshan, M. S.; Zhao, D.; Zhang, F. Elemental Migration in Core/Shell Structured Lanthanide Doped Nanoparticles. *Chem. Mater.* **2019**, *31*, 5608−5615.
(38) Hudry, D.; Busko, D.; Popescu, R.; Gerthsen, D.; Abeykoon, A. M. M.; Kübel, C.; Bergfeldt, T.; Richards, B. S. Direct Evidence of Significant Cation Intermixing in Upconverting Core@Shell Nanocrystals: Toward a New Crystallochemical Model. *Chem. Mater.* **2017**, *29*, 9238−9246.

https://doi.org/10.1021/acs.nanolett.3c01621
Nano Lett. 2023, 23, 7221−7227